Available online at www.sciencedirect.com
SCIENCE DIRECT
International Journal of Heat and Mass Transfer 49 (2006) 905–918
International Journal of HEAT and MASS TRANSFER
www.elsevier.com/locate/ijhmt

# The thermal characteristics of a hot wire in a near-wall flow

Li Wenzhong [a], B.C. Khoo [a,b,*], Xu Diao [c]

[a] Department of Mechanical Engineering, National University of Singapore, Kent Ridge, Singapore 119260, Singapore
[b] Singapore-MIT Alliance, 4 Engineering Drive 3, Singapore 117576, Singapore
[c] Institute of High Performance Computing, 1 Science Park Road, #01-01 The Capricorn, Singapore Science Park II, Singapore 117528, Singapore

Received 16 April 2004; received in revised form 15 May 2005
Available online 21 November 2005

**Abstract**

A two-dimensional numerical study is carried out to obtain the correction curve for the near-wall measurements by an infinitely long hot wire having been calibrated under free stream condition for the two extreme cases of isothermal and adiabatic wall conditions. Unlike previous studies particularly in experiments where the correction curve is primarily based on only the distance ($h$) between the wall and the wire expressed in wall units ($Y^+ \equiv \frac{hU_\tau}{\nu}$), it is found that a second dimensionless parameter $h_0$ ($\equiv h/D$) accounting for the effect of the hot wire diameter ($D$) is necessary to describe fully the overall near-wall correction curve. Our calculations also reveal a possible reason for the apparent discrepancy between the near-wall hot wire correction curves of Chew and Shi [Y.T. Chew, S.X. Shi, Wall proximity influence on hot-wire measurements, In: R.M.C. So, C.G. Speziale, B.E. Launder (Eds.), Near-Wall Turbulent Flows, Elsevier, Amsterdam, 1993, pp. 609–619] and Lange et al. [C.F. Lange, F. Durst, M. Breuer, Wall effects on heat losses from hot-wires. Int. J. Heat Fluid Flow 20 (1999) 34] next to a thermally non-conducting wall.


*Keywords:* Hot wire correction factor; Near-wall measurement; Critical $Y_c^+$; Overheat ratio

## 1. Introduction

In Perry and Morrison [3], it was found that their hot wire system with the DANTEC-made CTA operating under free stream condition has a frequency of well over 5 kHz when subject to direct velocity perturbations via the Karman vortex shed from one side of the cylinder. The said frequency response agreed well with the conventional square-wave voltage perturbation tests, which indicates a roll-off frequency of 5 kHz. Subsequent model/theory put forth by Freymuth [4] has shown the near-equivalence between the velocity and voltage perturbation tests in determining the dynamic response of the hot wire system. The square-wave voltage perturbation test, thus, has been used extensively and almost exclusively by experimentalists to justify the very rapid thermal response of the hot wire in faithful measurement of the fluctuating velocity in a turbulent flow with its typical range of frequency expected [5,6]. That is, a hot wire having been calibrated under imposed mean free stream condition can be employed for fluctuating velocity measurement. This practice is incumbent on the heat transfer characteristics of hot wire as exposed in the measured flow to be the same as that during the calibration. Such assumption, however, is no longer valid when the same hot wire is used in near-wall measurements. The wall may change the heat transfer characteristics of the hot wire with its calibration curve obtained under free stream condition, since more or even less heat is released from the hot wire due to the influence of wall effects. Therefore, some corrections on the measured velocity are needed for the near-wall measurement for the hot wire having been calibrated under free stream (wall-remote) flow condition. The problem was studied experimentally by numerous researchers over the years like Wills [7], Oka and Kostic [8], Singh and Shaw [9], Hebber

* Corresponding author. Address: Department of Mechanical Engineering, National University of Singapore, Kent Ridge, Singapore 119260, Singapore. Tel.: +65 68742889; fax: +65 67791459.
*E-mail address:* mpekbc@nus.edu.sg (B.C. Khoo).

0017-9310/$ - see front matter © 2005 Elsevier Ltd. All rights reserved.
doi:10.1016/j.ijheatmasstransfer.2005.06.044

**Nomenclature**

| | |
|---|---|
| $C_d$ | drag coefficient |
| $C_u$ | correction factor $= \frac{U_0}{U_{meas}}$ |
| $C_{ua}$ | correction factor for adiabatic wall case |
| $C_{ui}$ | correction factor for isothermal wall case |
| $D$ | diameter of hot wire |
| $du^+$ | correction factor $= \frac{U_{meas}-U_0}{U_\tau}$ |
| $d^+$ | Reynolds number $= \frac{U_\tau D}{\nu}$ |
| $Ec$ | Eckert number $= \frac{U_0^2}{C_P(T_w-T_\infty)}$ |
| $Gr$ | Grashof number $= \frac{g\beta(T_w-T_\infty)D^3}{\nu_\infty^2}$ |
| $H$ | the distance from the center of the hot wire to the wall |
| $H'$ | heat flux through the closed circulation which surrounds the cylindrical hot wire |
| $H_0$ | the non-dimensional distance from the center of the hot wire to the wall $= \frac{h}{D}$ |
| $L$ | hot wire length |
| $N_u$ | Nusselt number |
| $N_{u0}$ | Nusselt number obtained under free stream operating condition |
| $N_{um}$ | measured Nusselt number |
| $N_{uf}$ | Nusselt number ($N_{u0}$) based on fluid properties evaluated at the film temperature |
| $Pe$ | Peclet number $= Re\,Pr$ |
| $Pr$ | Prandtl number $= \frac{\mu_\infty Cp_\infty}{k_\infty}$ |
| $Re$ | Reynolds number $= \frac{U_0 D}{\nu_\infty}$ |
| $Re_f$ | Reynolds number based on fluid properties evaluated at the film temperature |
| $T$ | temperature |
| $U_0$ | the (true) upstream incoming flow velocity at the location of hot wire center |
| $U_{meas}$ | measured velocity value |
| $U_\tau$ | friction velocity |
| $Y^+$ | non-dimensional wall distance $= \frac{hU_\tau}{\nu} \equiv h_0 \frac{U_\tau D}{\nu}$ |
| $Y_c^+$ | critical $Y^+$, beyond which wall influence can be neglected |

*Greek symbols*

| | |
|---|---|
| $\varepsilon_f$ | maximum difference between the respective values of stream function on successive iterations |
| $\varepsilon_v$ | maximum difference between the respective values of vorticity on successive iterations |
| $\varepsilon_t$ | maximum difference of the temperature on successive iterations |
| $\nu$ | kinematic viscosity |
| $\tau$ | overheat ratio ($\equiv T_w/T_\infty$) |

*Subscripts*

| | |
|---|---|
| $\infty$ | at the inlet of computational domain |
| w | conditions at the hot wire |

[10], Krishamoorthy et al. [11] and Chew et al. [12], to name a few. Numerically, Bhatia et al. [13], Chew and Shi [1] and Lange et al. [2,14], have tried to find a suitable universal correction for the near-wall hot wire measurements velocity, but met with limited success and in some instances presented conflicting trends.

In early hot wire applications, Van der Hegge Zijnen [15] measured the heat loss of the hot wire in still air near the wall as the required correction quantity to the measured signal for the flowing air in the near-wall region. Wills [7] introduced the term $k_w(2y/D)$ to account for the wall effect in his experimentally obtained wall corrections relationship for laminar flow:

$$N_u\left(\frac{T_w}{T_a}\right)^{-0.17} = A + k_w\left(\frac{2y}{D}\right) + B * Re_D^{0.45}. \quad (1)$$

Here $k_w$ is the ratio of the thermal conductivity of wall material to the thermal conductivity of air; $y$ is the distance of hot wire from the wall; $D$ is the wire diameter; $N_u$ is the Nusselt number; $Re_D$ is Reynolds number based on wire diameter, and $A$ and $B$ are arbitrary constants. One may also note that Collis and Williams [16] fitted their experimental data in the range of Reynolds number from 0.02 to 44 on the curve:

$$N_u\left(\frac{T_f}{T_a}\right)^{-0.17} = 0.24 + 0.56\,Re_D^{0.45} \quad (2)$$

where the fluid properties were evaluated at the film temperature, $T_f$ ($\equiv(T_{wire} + T_a)/2$), the mean of hot wire and ambient air temperature. On comparing the two equations, it is clear that Eq. (1) implies the additional heat loss due to the presence of the wall is (or can be) determined by the dimensionless parameter $h_0$ ($\equiv y/D \equiv h/D$). For turbulent flow measurement, Wills [7] suggested that only half of the correction for laminar flow should be employed. However, no explanation, whether physical or otherwise, is given.

Still, Oka and Kostic [8] and Hebbar [10] obtained the corrections from measurements in turbulent channel and boundary layer flows, respectively, and suggested that the correction can universally collapsed to a single curve $\Delta U^+ = f(Y^+)$. Here $\Delta U^+$ and $Y^+$are defined as

$$\Delta U^+ = \frac{U_{meas} - U_0}{U_\tau} \quad (3)$$

$$Y^+ = \frac{yU_\tau}{\nu} \quad (4)$$

where $U_{meas}$ is the measured apparent velocity, $U_0$ is the actual velocity, and $U_\tau$ is the wall shear velocity. Such a cor-

rection curve seems to imply that the near-wall effect is (at least directly) independent of Reynolds number and wire diameter.

Krishnamoorthy et al. [11] carried out experimental investigation on the influence of wire diameter and temperature loading on the near-wall velocity correction factor. They suggested that the increase of the hot wire diameter and temperature loading give rise to a larger correction at a given $Y^+$, which implies that the correction is not exclusively a function of the non-dimensional wall distance $Y^+$. Still Singh and Shaw [9] pointed out that the correction is independent of wall conductivity, while Polyakov and Shindin [17] and Zemskaya et al. [18] showed otherwise the importance of wall thermal conductivity. And perhaps Bruun [19] has aptly summed up with the remark that "...no universal correction curve or procedure has been established ..." thus far.

Due to the inherent experimental difficulties of accurate near-wall measurements and limitations of varying the numerous parametric operating conditions, numerical experiment to study the near-wall effects appears to be an attractive alternative especially with the advent of powerful computer and new computational methodology. One of the first from Bhatia et al. [13] considered the simplified model with the wire taken as a line source. Hence wire diameter influence on the correction of hot wire was ignored; however, Krishnamoorthy et al. [11] experimentally showed that diameter influence is an important consideration for near-wall correction.

Among the other numerical studies to find the near-wall measurement correction curves, Chew and Shi [1] and Lange et al. [2,14] conducted fairly extensive works. Although both obtained similar near-wall hot wire correction curve for conducting wall with isothermal boundary condition, their respective hot wire correction curve exhibit completely opposite trend for non-conducting wall of adiabatic thermal boundary condition. Chew and Shi [1] showed that for the non-conducting wall, as the hot wire is positioned increasingly close to the wall, the heat loss from the wire remains higher than the corresponding case without the presence of the wall; they attributed this phenomenon to the distortion of velocity field by the wall and consequent alteration of the heat transfer characteristics of the hot wire such that there is an overall larger heat loss to the flow. On the other hand, Lange et al. [2] pointed out that for a perfectly insulating wall material, "...the diffusive heat flux perpendicular to the main flow that would occur in a free stream is suppressed. This suppression causes an accumulation of heat between the cylinder and the wall, reducing the temperature gradient in this region ...", and hence leading to a reduction in the measured Nusselt number. This discrepancy in the trend observed is but perhaps not unexpected since there are several different factors which may influence the results, like the domain size employed, the convergence criteria and assumptions concerning the physical properties of the fluid such as use of the mean film temperature and others. A more extensive investigation is required to resolve this discrepancy.

This work is aimed at using a reasonable domain size for computation and to resolve the discrepancy of trend as observed between Chew and Shi [1] and Lange et al. [2] by solving the coupled Navier–Stokes equation with the energy equation in a two-dimensional flow via control volume method. Further, some of the important parameters like wall conductivity, wire diameters, distance from the wall, overheat ratio on the near-wall measurement are systematically investigated and their respective influences compared. Finally the correction curves for (universal) applications to near-wall hot wire measurements based on the main dimensionless parametric groupings are obtained.

## 2. Governing equations and boundary conditions

The following assumptions and considerations are adopted in the numerical analysis:

1. The fluid flow and heat transfer are regarded as incompressible, steady, 2-D flow past an infinitely long circular wire that is aligned parallel to the wall and normal to the flow. This consideration was based on Azad [20], which showed that for measurements within the viscous sublayer with a single normal probe, the wire must be straight and parallel to the wall.
2. The wire is subjected to an inflow shear velocity field varying linearly with the distance from the wall similar to a viscous sublayer flow.
3. The properties of fluid, like viscosity, thermal conductivity, etc., are taken as fully temperature dependent. The body force is accounted for as in Boussinesq's assumption.
4. Natural convection and viscous heating are included, and the direction of gravity is in the vertical direction and perpendicular to the coming flow.

The flow past a cylinder in the domain is depicted in Fig. 1. Boundary $B1$ is the inflow boundary, $B2$ is the top boundary, $B3$ is the wall boundary, $B4$ is the outflow

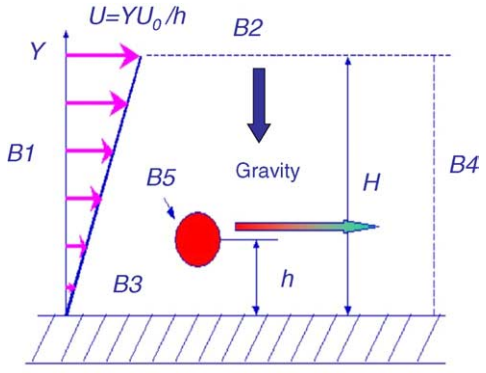


Fig. 1. Schematic drawing of the computational region.

boundary and boundary, $B5$ is the surface of hot wire. $H$ stands for the distance between top boundary ($B2$) and wall boundary ($B3$), while $h$ is the distance between the center of hot wire to the wall boundary ($B3$).

Taking the diameter of hot wire $D$ as the characteristic length, the upstream flow velocity at the wire location ($U_0$) as the characteristic velocity, the following dimensionless variables (as indicated by the '*' sign) are:

$$x^* = \frac{x}{D} \quad u^* = \frac{u}{U_0} \quad p^* = \frac{p}{\rho_\infty U_0^2}$$
$$T^* = \frac{(T - T_\infty)}{(T_w - T_\infty)} \quad \mu^* = \frac{\mu}{\mu_\infty} \quad k^* = \frac{k}{k_\infty}$$

Here the subscript '$\infty$' denotes the condition at the upstream location and the variables denote the usual meanings. The non-dimensionalised governing equations of continuity, momentum and energy can be expressed respectively as follows:

Continuity equation:

$$\frac{\partial}{\partial x_i^*}(u_i^*) = 0 \quad i = 1, 2 \tag{5}$$

Momentum equations:

$$u_i^* \frac{\partial}{\partial x_i^*}(u_j^*) = \frac{\partial p^*}{\partial x_j^*} + \frac{1}{Re}\frac{\partial}{\partial x_i^*}\left[\mu^*(T^*)\frac{\partial u_j^*}{\partial x_i^*}\right] + \left(\frac{Gr}{Re^2}\right)T^* \quad i = 1, 2 \tag{6}$$

Energy equation:

$$\frac{\partial}{\partial x_i^*}\left(u_i^* T^*\right) = \left(\frac{1}{Re * Pr}\right)\frac{\partial}{\partial x_i^*}\left[k^*(T^*)\frac{\partial T^*}{\partial x_i^*}\right] + \frac{Ec}{Re}\cdot \Phi^* \quad i = 1, 2 \tag{7}$$

Here $u_i$ and $x_i$ are the Cartesian velocity components and coordinates, respectively. The dissipation function is

$$\Phi^* = \left(\frac{\partial u_i^*}{\partial x_j^*} + \frac{\partial u_j^*}{\partial x_i^*}\right)\frac{\partial u_i^*}{\partial x_j^*} \tag{8}$$

where $\mu^*$ is the dimensionless dynamic viscosity given by

$$\mu^* = [T^*(\tau - 1) + 1.0]^{\frac{3}{2}}\left(\frac{1 + \frac{S_\mu}{T_\infty}}{(T^*(\tau - 1) + 1.0) + \frac{S_\mu}{T_\infty}}\right) \tag{9}$$

and $k^*$ is the dimensionless thermal conductivity of fluid such that

$$k^* = [T^*(\tau - 1) + 1.0]^{\frac{3}{2}}\left(\frac{1 + \frac{S_k}{T_\infty}}{(T^*(\tau - 1) + 1.0) + \frac{S_k}{T_\infty}}\right) \tag{10}$$

One may note that both $\mu^*$ and $k^*$ are based on Sutherland Formula [21] which expresses how the physical properties of fluid changes with the temperature as reflected in $\tau$ ($\equiv T_w/T_\infty$, the overheat ratio of hot wire). $S^\mu$ and $S^k$ are effective temperatures called the Sutherland constants, which are characteristic of the gas. For air, $S^\mu$ and $S^k$ are taken as constants at 111 K and 194 K, respectively.

Eqs. (5)–(7) reveal the dimensionless parameters affecting the flow field and heat transfer characteristic as Reynolds number ($Re \equiv \frac{U_0 D}{\nu_\infty}$), Prandtl number ($Pr \equiv \frac{\mu_\infty C_P}{k_\infty}$), Grashof number ($Gr \equiv \frac{g\beta(T_w - T_\infty)D^3}{\nu_\infty^2}$), and Eckert number ($EC \equiv \frac{U_0^2}{C_P(T_w - T_\infty)}$).

The average Nusselt number is defined as

$$N_u = \frac{1}{A}\oint \frac{qD}{k(T_w - T_\infty)}\,\mathrm{d}A = \frac{H'}{\pi k(T_w - T_\infty)} \tag{11}$$

where $H'$ is the heat flux through the closed circulation which surrounds the cylindrical hot wire.

The corresponding dimensionless boundary conditions in Fig. 1 are as follows:

$B1$: $x^* = x_s^* \quad u^*(y^*) = (u_0^*/h^*)y^* \quad v^* = 0 \quad T^* \equiv T_\infty^* = 0$

$B2$: $y^* = H^* \quad u^* = (u_0^*/h^*)H^* \quad v^* = 0 \quad T^* \equiv T_\infty^* = 0$

$B3$: $y^* = 0 \quad u^* = 0 \quad v^* = 0,$

$T^* \equiv T_\infty^* = 0$ isothermal or $\frac{\partial T^*}{\partial y^*} = 0$ adiabatic

$B4$: $x^* = x_e^* \quad \partial u^*/\partial x^* = \partial v^*/\partial x^* = 0 \quad \partial T^*/\partial x^* = 0$

$B5$: $u^* = v^* = 0 \quad T^* \equiv T_{\text{wire}}^* = 1.0$

## 3. Numerical calculations: grid distribution and size of computational domain

For the spatial discretization of governing equations (5)–(7), the finite volume method with a collocated arrangement of the variables was employed. Eqs. (6) and (7) are integrated over each control volume, leading to a balance equation for the fluxes through the control volume faces and the volumetric sources. The fluid properties in Eqs. (6) and (7) are calculated as functions of temperature by Sutherland Formula defined in Eqs. (9) and (10), and updated at each new iteration. The diffusion contributions to the fluxes are evaluated using a second order central differencing scheme, while the convection contributions to the fluxes are evaluated using the second order upwind differencing scheme to reduce the effects of numerical diffusion on the solution. For the pressure calculation, a pressure correction equation is used instead of Eq. (6) and was solved iteratively with Eq. (7) following the SIMPLEC algorithm [22]. Unless otherwise stated, convergence criteria are achieved when the maximum of the normalized absolute residuals in all equations is reduced to a value below $10^{-6}$. Details of the numerics and implementation are available in the works of Li [23].

### 3.1. Grid distribution

On the grid distribution, the 'eye' type grid distribution surrounding the hot wire as depicted in Fig. 2 is adopted. Near to the wall, the grid distribution is much finer to resolve the intricate flow features as expected. The grid is non-uniform, and has locally refined features around the cylinder to obtain better resolution of flow field near the

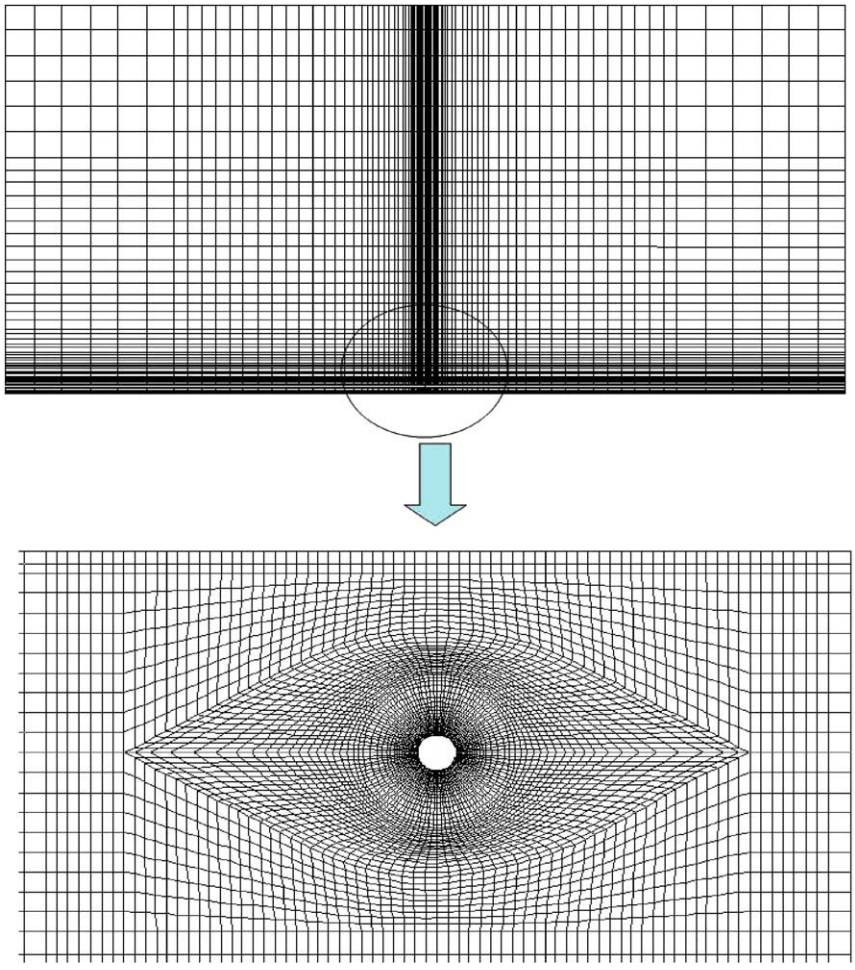

Fig. 2. The grid distribution near the wall and the around the hot wire.

cylinder. The grid lines are closely aligned with the flow direction as based on the analysis of De Vahl Davis and Mallinson formula (refer to [24]).

The grid and computational domain independent checks are similar to that carried out in Li et al. [25]. Briefly, there is the grid independent check of the nodes distribution around the hot wire resulting in the employment of 120 grid points in this work throughout. On the size of the computational domain, based on the above grid distribution and the minimum typical Reynolds number for near-wall hot wire measurement, the initial domain size of $20D \times 20D$ with the hot wire at the centre is increased until the computed drag coefficient and Nusselt number are essentially invariant with further increase in the domain size. The test case is for Reynolds number $= 1.5 \times 10^{-2}$; the temperature of cylinder wall $T_w = 301$ K, and the temperature of free stream $T_0 = 300$ K. Correspondingly, the overheat ratio of hot wire ($\tau$) is 1.003, so the influence of temperature-dependent properties can be neglected. The results obtained are given in Table 1. It is found that a dimension of $1300D \times 1300D$ would give rise to a computed Nusselt number differing less than about 0.2% from the quantity calculated with the much larger dimension of $4000D \times 4000D$. Lange [26] has largely employed a domain in excess of $4000D \times 4000D$ and a typical Nusselt number evaluated at $Re = 0.015$ gives rise to 0.31627 which concurs with our calculated quantity of 0.31685 to within 0.1%. In this work, a domain measuring $1300D \times 1300D$ is used throughout unless otherwise stated.

Table 1
Variation of $C_d$ and $N_u$ with domain size for $Re = 1.5 \times 10^{-2}$

| Case ($n$) | Domain size | Drag coefficient ($C_d$) | Nusselt number ($N_u$) |
|---|---|---|---|
| 1 | $20D \times 20D$ | $7.3089 \times 10^2$ | 0.41082 |
| 2 | $100D \times 100D$ | $4.3401 \times 10^2$ | 0.33446 |
| 3 | $200D \times 200D$ | $3.7049 \times 10^2$ | 0.32326 |
| 4 | $400D \times 400D$ | $3.2617 \times 10^2$ | 0.32004 |
| 5 | $800D \times 800D$ | $2.9798 \times 10^2$ | 0.31855 |
| 6 | $1300D \times 1300D$ | $2.8617 \times 10^2$ | 0.31721 |
| 7 | $4000D \times 4000D$ | $2.7838 \times 10^2$ | 0.31685 |

## 4. Heat transfer from a circular cylinder in (free stream) uniform flow

Based on the grid distribution and computation domain size of $1300D \times 1300D$, the heat loss from a

circular cylinder in uniform flow was computed at the low Reynolds number range normally encountered in equivalent near wall hot wire measurements. For comparison, the results in terms of Nusselt number ($N_{uf}$, based on fluid properties evaluated at the film temperature) verses Reynolds number ($Re_f$, also based on fluid properties evaluated at the film temperature) at the overheat ratio of 1.5 are presented in Fig. 3 with Oseen's solution, Kramer's (experimental) formula for Reynolds number ranging from 0.1 to 40,000, and the empirical formula based on experiments put forth by Collis and Williams [16]. Also shown is the numerical prediction by Lange et al. [27]. Our results are lower than those given by Kramer's formula. The discrepancies may be caused by the three-dimensional effect encountered in experiments; such effect is absent in the present two-dimensional calculation. When compared to the formula of Collis and Williams [16], our computed Nusselt number assumes only a slightly smaller quantity for $Re_f < 0.03$ and shows a slightly faster increase with $Re_f > 0.03$. Our results agree well with Oseen's solution for Reynolds number less than 0.025, but the deviation increases with increasing Reynolds number, which can be attributed to the failure/limitation of linear assumption in Oseen's solution. Compared with the result of Lange et al. [27], our $N_{uf}$ agrees very well with only a very marginally higher value at the lower Reynolds number range. This discrepancy can perhaps be attributed to the neglect of natural convection term in the simulation by Lange et al. [27]. Generally, the reasonable agreement with experimental and numerical results augers well for our theoretical formulation and numerical method adopted in the present work.

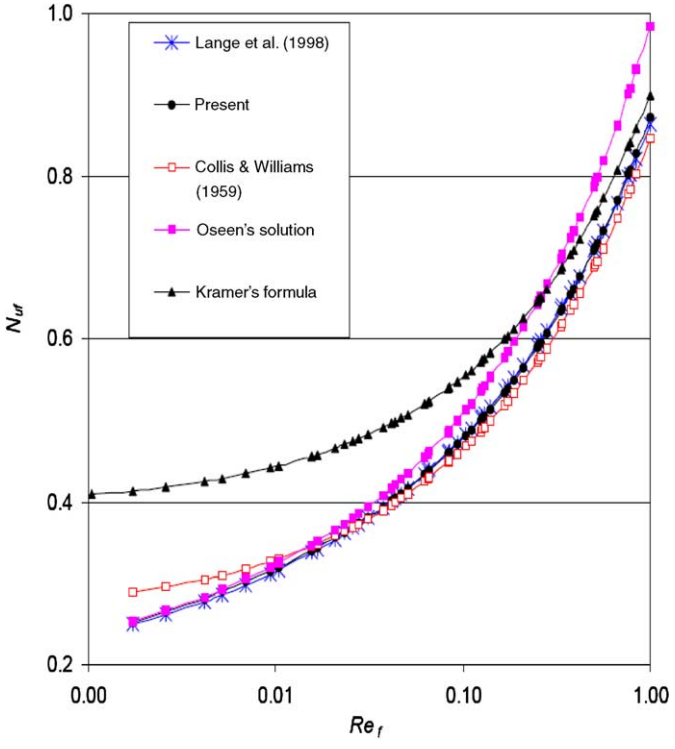


Fig. 3. Heat transfer from a circular cylinder in a free stream uniform flow for $\tau = 1.5$.

Based on the above numerical simulation results of hot wire heat transfer from a circular cylinder in a steady flow, one can always obtain the calibration equation for the velocity pertaining to the hot wire under free stream conditions and use as a reference against which subsequent calculations with wall effects are compared to in order to obtain the near-wall corrections for various near-wall hot wire measurements.

## 5. Thermal response of a hot wire in a near-wall flow

### *5.1. Plausible causes for the discrepancy between the near-wall hot wire correction curves of Chew and Shi and Lange et al. for adiabatic wall*

Chew and Shi [1] and Lange et al. [2] carried out simulations of near-wall hot wire measurement. From their results, it is found that the correction curve trend is identical for near-wall hot wire operation near fully thermal-conducting (isothermal) wall while for the non-conducting (adiabatic) wall, the trend is totally different. Chew and Shi's results showed that as the hot wire is positioned close to the adiabatic wall, the heat loss from the wire is still greater than the corresponding case without the wall; this trend of greater heat loss is found similar to the arrangement of isothermal wall (see also [28]). In their work, Chew and Shi [1] did not provide details of the computed temperature distribution of the flow field with and without the wall for comparison, nor present calculation of the heat flux from the hot wire to indicate a larger proportion of heat loss has occurred in the region between the wire and the wall. They, however, used their experimental data obtained for hot wire operation near an aluminum (thermally more conducting) and perspex (thermally less conducting) wall and showed that these experiments lies between the extreme limit of their computations for isothermal and adiabatic walls. On the other hand Lange et al. suggested the insulating wall would suppress the flow and cause an accumulation of heat between the hot wire and the wall thereby reducing the temperature gradient in this region. This would result in a reduction of the measured Nusselt number. In fact, there was also mentioned made of the opposite trend observed in Chew and Shi but no further discourse to resolve the apparent discrepancy by Lange et al. [14]. The following calculations were carried out to find the cause of the above-mentioned discrepancy between the results of Chew and Shi and Lange et al., and more importantly to establish the correct trend.

There were several differences in parameter setting between Chew and Shi and Lange et al., such as the wall friction velocity $U_\tau$, hot wire overheat ratio, natural convection, viscous heating as well as the computational domain size. Each factor was studied and quantified in terms of the respective contribution to the accuracy of the computation. It is found that each factor only made

a limited contribution of less than 5% in terms of the evaluated Nusselt number and hence is deemed unlikely to cause a complete change of the trend of the near-wall correction curve. (Details of the comparison for each factor are available in [23]). Even the employment of a relatively very much smaller computational domain of 150D in front and top of the cylinder, and 240D to the rear of the cylinder by Chew and Shi as compared to a domain of $4000D \times 4000D$ is limited to a difference of about 2% for $N_u$.

Several computational runs were carried out to ascertain if setting the convergence criterion $\varepsilon_f$ (maximum difference between the respective values of stream function on successive iterations) and $\varepsilon_v$ (maximum difference between the respective values of vorticity on successive iterations) to be less than $1.0 \times 10^{-4}$ is sufficiently good as used in Chew and Shi [1]. A typical configuration with $Re = 0.15$, the distance of hot wire to the wall $h_0 (\equiv h/D) = 1.5$, a shear velocity of $U_\tau = 1.0$ m/s giving rise to $Y^+ (\equiv hU_\tau/v) = 0.5$ and an overheat ratio $\tau = 1.8$ was employed. The computed $N_u$ based on several under-relaxation factors for temperature are tabulated in Table 2. It is apparent that with $\varepsilon_f$ and $\varepsilon_v = 1.0 \times 10^4$, $N_u$ varies with the temperature under-relaxation factor; this should not be the case as the intent of relaxation factor serves to stabilize the iteration process but not alter the result. Incidentally in Chew and Shi's simulation, an under-relaxation factor was employed in conjunction with $\varepsilon_f$ and $\varepsilon_v = 1.0 \times 10^{-4}$. Also shown in Table 2 are the computed $N_u$ based on the more stringent criterion of $\varepsilon_f$, $\varepsilon_v$ and $\varepsilon_t = 1.0 \times 10^{-6}$ which indicates independence of the under-relaxation factor employed. It is suggested therefore that the use of an insufficiently stringent convergence criterion has probably resulted in the perceived discrepancy of trend between Chew and Shi [1] and Lange et al. [2] for the case of non-conducting wall.

One particularly interesting point to note is that for isothermal wall case, though the convergence criterion for $\varepsilon_f$, $\varepsilon_v = 1.0 \times 10^{-4}$ as used by Chew and Shi [1] is not stringent enough to get the convergent result, it is fortuitous that the ratio $N_{u0}/N_u$ (or interpreted as the velocity correction factor) obtained still showed a similar trend as for Lange et al. [2,14]. Table 3 shows the computed $N_u$ based on different convergence criterion and employment of various under-relaxation factor for temperature. One can note that the variation of $N_u$ is much smaller and limited to below 5%, which may be a possible reason for the fortuitous concurrence of velocity correction factor trend between Chew and Shi [12] and Lange et al. [2,14]. In all our simulations, we ascertain convergence not only by examining residual levels and $\varepsilon_f$, $\varepsilon_v$, $\varepsilon_t$ to be less than $1.0 \times 10^{-6}$ but also by monitoring relevant integrated quantities that are of pertinent interest, such as drag or heat transfer coefficient.

### 5.2. Main parameters affecting the near-wall hot wire correction factor

In Chew and Shi [1] and Lange et al. [2,14], it was implicitly and broadly suggested that there could be a

Table 2
$N_u$ for $Y^+ = 0.5$, $U_\tau = 1.0$ m/s, $Re = 0.15$, $\tau = 1.8$ ($N_{u0} = 0.495$) for adiabatic wall

| $\varepsilon_f$, $\varepsilon_v$, $\varepsilon_t$ | Under-relaxation factor for temperature | Nusselt number | $\frac{N_{u0}}{N_u}$ (or $C_u$) | Remarks: simulated result exhibit similar trend as |
|---|---|---|---|---|
| $1.0 \times 10^{-4}$ | 1.00 | 0.46845 | >1.0 | Lange et al. |
| | 0.80 | 0.64628 | <1.0 | Chew and Shi |
| | 0.65 | 0.70000 | <1.0 | Chew and Shi |
| | 0.60 | 0.80074 | <1.0 | Chew and Shi |
| $1.0 \times 10^{-6}$ | 1.00 | 0.46014 | >1.0 | Lange et al. |
| | 0.80 | 0.46014 | >1.0 | Lange et al. |
| | 0.65 | 0.46017 | >1.0 | Lange et al. |
| | 0.60 | 0.46020 | >1.0 | Lange et al. |

Table 3
$N_u$ for $Y^+ = 0.5$, $U_\tau = 1.0$ m/s, $Re = 0.15$, $\tau = 1.8$ ($N_{u0} = 0.495$) for isothermal wall

| $\varepsilon_f$, $\varepsilon_v$, $\varepsilon_t$ | Under-relaxation factor for temperature | Nusselt number | $\frac{N_{u0}}{N_u}$ (or $C_u$) | Remarks: simulated result exhibit similar trend as |
|---|---|---|---|---|
| $1.0 \times 10^{-4}$ | 1.00 | 1.17082 | <1.0 | Lange et al. |
| | 0.80 | 1.18164 | <1.0 | Chew and Shi |
| | 0.65 | 1.19543 | <1.0 | Chew and Shi |
| | 0.60 | 1.21362 | <1.0 | Chew and Shi |
| $1.0 \times 10^{-6}$ | 1.00 | 1.17103 | <1.0 | Lange et al. |
| | 0.80 | 1.17103 | <1.0 | Lange et al. |
| | 0.65 | 1.17132 | <1.0 | Lange et al. |
| | 0.60 | 1.17181 | <1.0 | Lange et al. |

universal correction curve, which is a function of wall conductivity and $Y^+$. It was, however, also discussed in Chew and Shi [1] the influence of wire diameter in the correction curve, which would have implicitly acknowledged that an additional dimensionless parameter may be required for a fuller description of the near-wall correction factor. Our numerous simulations showed that the correction curve is not only a function of wall conductivity and $Y^+$, but also a function of wall distance $h_0$. This is perhaps not unexpected since the size of the wire diameter in relation to proximity to the wall will have some bearings on the flow aerodynamics between the wire and the wall and hence the associated heat transfer characteristic of the wire. From the non-dimensional N–S equations and energy equation, we know that heat transfer is influenced by *Re*, *Pr*, *Gr* and *Ec*. In the respective range for hot wire application, *Gr*, *Ec* and *Pr* have relatively small influence on $N_u$. Only the *Re* has a major influence on $N_u$. As *Re* can be determined or described fully by $Y^+$ and $h_0$ in the near-wall arrangement, this may suggest that $Y^+$ and $h_0$ are the major parameters influencing $N_u$ and hence the correction factor ($C_u$).

In our simulation, we firstly set $Y^+$ to be constant at 5, and the value of $h_0$ ($\equiv h/D$) is varied from 5, 10, 15, 30, 60, 90 to 150; the corresponding velocity correction factor for both adiabatic wall and isothermal wall is obtained. The overheat ratio ($\tau$) is 1.8. The results of the computation are given in Fig. 4, which shows that when $Y^+$ is kept constant, both $C_u$ increase with the increase of $h_0$. $C_u$ is the velocity correction factor, and defined as

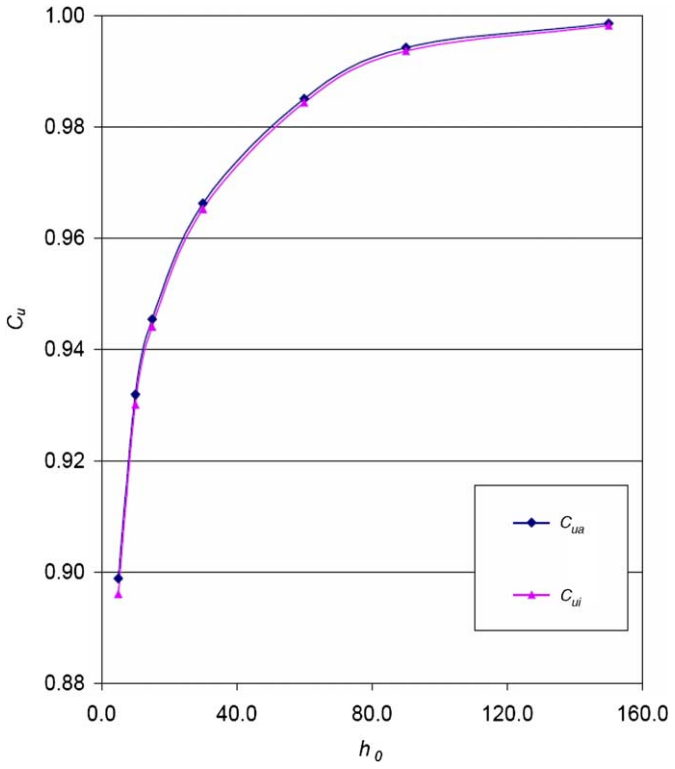


Fig. 4. Variation of $C_u$ with $h_0$ for $Y^+ = 5.0$.

$$C_u = \frac{U_0}{U_{\text{meas}}} \tag{12}$$

where $U_0$ is the upstream flow velocity at the wire center and $U_{\text{meas}}$ is the measured velocity. $U_{\text{meas}}$ is obtained by applying the calculated $N_u$ to the 'calibration curve' of $N_u$ versus *Re* for a hot wire under free stream operating condition (i.e. an equivalence of Fig. 3 for $\tau = 1.8$). (One may note that such is the procedure in experiment where $U_{\text{meas}}$ is obtained from the calibration curve nominally expressed as $E(\text{voltage}) = f(u)$ determined under free stream condition.)

In particular $C_{ua}$ stands for the correction factor pertaining to the adiabatic wall while $C_{ui}$ is the correction factor for the isothermal wall. Fig. 4 showed that the two velocity correction factor curves collapse into one single curve. This has an important implication. At $Y^+ \geqslant 5$, there is hardly any difference between the heat loss from the wire under either the thermally conducting or adiabatic wall. Also as $h_0$ increases beyond about 150, the influence of wall effect becomes negligible as $C_u$ approaches 1.0. From Fig. 4 we can surmise that $Y^+$ and $h_0$ are the main parameters, which affect the velocity correction factor $C_u$. (Alternatively, instead of $h_0$, an equivalent factor can be expressed as $d^+$ ($\equiv \frac{U_\tau D}{\nu}$) as pointed out by one reviewer.)

Based on these two main parameters identified, the variation of $C_{ui}$ and $C_{ua}$ are determined for a range of conditions. The variation is obtained for the typical hot wire operating at an overheat ratio of 1.8 and nominal ambient temperature of 300 K. Fig. 5 presents the $C_u$ versus $Y^+$ for various values of $h_0$. It is interesting to note that for $h_0 = 5$, although $C_u$ approaches 1.0 as $Y^+$ becomes larger, this only occurs for very large $Y^+$ beyond 10.0. It is prudent for one to bear this in mind for the case of smaller magnitude of $h_0$. This apparently contradicts various previous experimental results which show that wall influence is limited to $Y^+ = 5$ without any reference made to the possible effect of $h_0$. Closer examinations of some of these mentioned experiments indicate that $h_0$ was usually rather large at 40 or more when $Y^+ = 5$. For example, the laminar flow results obtained by Wills [7] correspond to $h_0$ at about 40 at $Y^+ = 5$. In the plot of $U^+$ versus $Y^+$ for the hot wire placed next to the aluminum wall in Fig. 12 of Chew et al. [12], their results show that at $Y^+ = 5$ the effect of wall influence becomes negligible; this corresponds to $h_0 \approx 40$. In other experiment to investigate the influence of wall proximity on hot wire velocity measurements, Oka and Kostic [8] kept their values of $h_0$ to about 60, which is sufficiently large to rule out significant $h_0$ effects when $Y^+ = 5$. Krishnamoorthy et al. [11] conducted experiments investigating effect of wire diameter and overheat ratio near an aluminum wall with $d^+$ ranging between 0.02 and 0.13. With a hot wire diameter of 5 μm, we can deduce that their $h_0$ is at least about 40 when $Y^+ = 5.0$.

Furthermore, from the plot of $N_u$ versus *Re* in their Fig. 2 for a 5 μm diameter wire at various heights near an aluminum wall, Chew et al. [12] observed that the wall

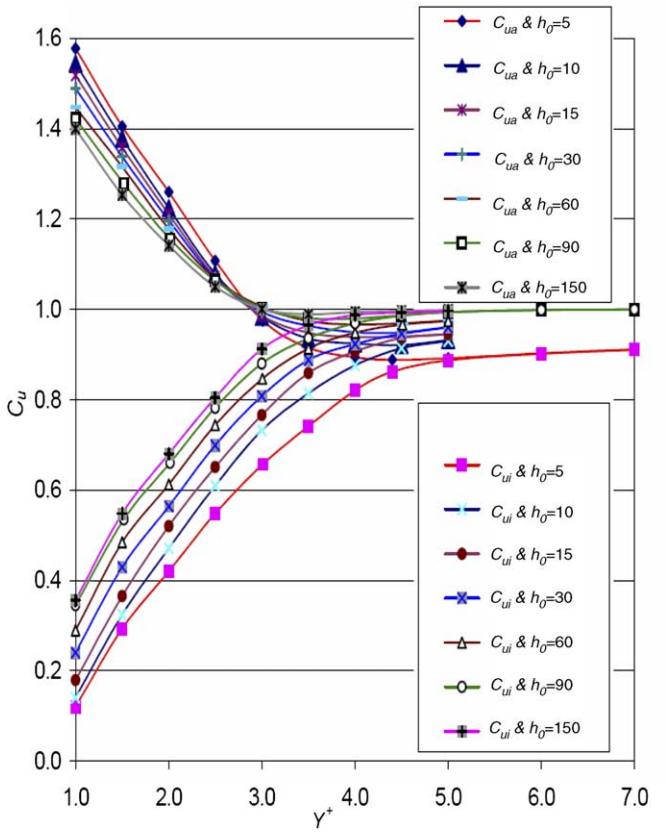


Fig. 5. Variation of $C_u$ with $Y^+$ and $h_0$ ($\tau = 1.8$).

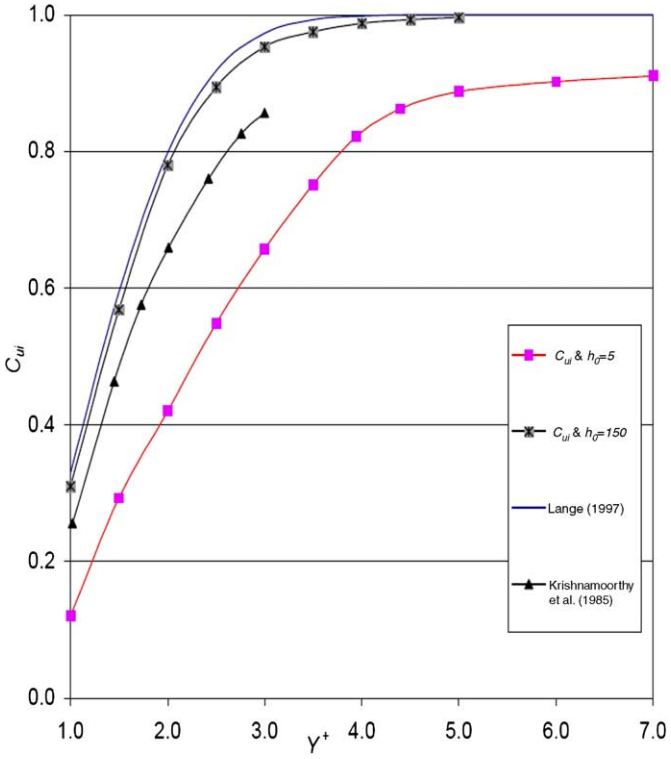


Fig. 6. Variation of $C_u$ with $Y^+$ and $h_0$ for isothermal wall ($\tau = 1.8$) with comparison to experiments [11].

influence can extend beyond $Y^+ \geqslant 5.0$, provided $h_0$ is sufficiently small. It is clear that for their range of smaller $h_0$, the distribution of $N_u$ does not coincide and only approaches the corresponding $N_u$ at free stream (taken to be the measurements at the center of the channel flow) at $Y^+$ beyond 5. Though the overheat ratio used at $\tau = 1.1$ is different from the overheat ratio at $\tau = 1.8$ in our simulation, the trend is still evident.

Shown in Fig. 6 is the experimental result of velocity correction factor for a 5 μm diameter hot wire placed near an aluminum wall at an overheat ratio of $\tau = 1.8$ from Krishnamoorthy et al. [11]. Krishnamoorthy et al. had given the original representation of the velocity corrections in the form of $\Delta U^+$ versus $Y^+$ as did by most other works like Oka and Kostic [8] and Chew and Shi [1]. However, in the viscous sublayer, since $U^+ = Y^+$, therefore the relation between $C_u$ and $\Delta U^+$ can be written as

$$\Delta U^+ = \frac{U_{\text{meas}} - U_0}{U_\tau} = \frac{U_0(\frac{1}{C_u} - 1)}{U_\tau} = \frac{Y^+ U_\tau \left(\frac{1}{C_u} - 1\right)}{U_\tau} = Y^+ \left(\frac{1}{C_u} - 1\right) \tag{13}$$

In Krishnamoorthy et al., the influence of $h_0$ is not stated explicitly though they deemed $h_0$ to be a parameter determining the effect of wall proximity. From Fig. 6, we can see that their $C_u$ lies rather neatly between the velocity correction curve of $h_0 = 5$ and $h_0 = 150$ from our calculations. It is noted that the different $h_0$ employed in the experiments are in the estimated range of $8 < h_0 < 40$, and not maintained as a constant. (In experiment, it is invariably not the intent of keeping $h_0$ constant as the hot wire traversed spatially across the viscous sublayer). In the same Fig. 6, $C_{ui}$ as taken from Lange [26] is reproduced here which corresponds quite closely to our simulated case of $h_0 = 150$. Lange also did not state explicitly the value of $h_0$ employed in the simulation. However, judging from the close correspondence of his results with our simulation at $h_0 = 150$, we may surmise that the $h_0$ employed is possibly rather large. This is inferred from our simulations where the variation of $C_{ui}$ with $Y^+$ at large $h_0$ is much more limited compared to the smaller $h_0$ values.

More detailed examination of the behavior of $C_u$ is shown next in Fig. 7 for selected $h_0$. It is observed that as $Y^+$ increases beyond about 4.0, $C_{ui}$ and $C_{ua}$ approach very close to each other. This may imply that the influence of the wall thermal conductivity becomes an essentially non-issue. (Although not shown in Fig. 7, this trend is the same for $h_0 = 10$, 15, 30 and 60.) Of course in the experiments, any real wall possesses a thermal conductivity, which should lie between the two extremes of adiabatic and isothermal walls.

A point worth mentioning from Fig. 7 is that as $Y^+$ increases from 1.0, $C_{ua}$ decreases from a value above 1.0 and goes slightly below 1.0 before rising towards 1.0 again. This magnitude of the deviation from below $C_u = 1.0$ at the

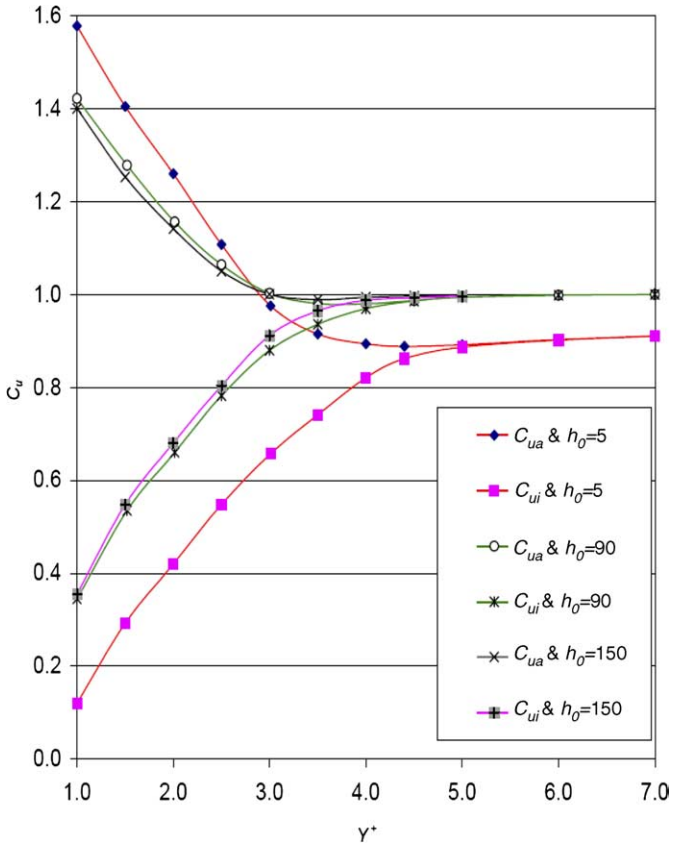


Fig. 7. Variation of $C_u$ with $Y^+$ and $h_0$ ($\tau = 1.8$).

turning point and the value of $Y^+$ when it occurs is dependent on $h_0$. The smaller the value of $h_0$, the larger the deviation of $C_{ua}$ below 1.0 is. Incidentally, Lange et al. [26] actually did obtain a few data points with $C_{ua} < 1.0$ in the vicinity of $Y^+ \approx 3.46$ (see also [2,14]). However, there is no further elaboration about this crossover of $C_{ua}$ below 1.0 except that it was remarked by Lange and coworkers [14,26] that "...The correction values calculated for the largest nondimensional wall distance $Y^+ = 3.46$ were obviously underestimated...". This is not surprising since their interest is largely confined to the lower range of $Y^+$ below 3.0 and there are hardly any calculations in the higher $Y^+$ range where this phenomenon is clearly observed. Also, if $h_0$ used in their calculation is large, this deviation of $C_{ua}$ below 1.0 becomes correspondingly smaller and not so easily discerned. Another feature from Fig. 7 is that for a given $h_0$, $C_{ua}$ approaches 1.0 faster than $C_{ui}$ as $Y^+$ increases. Since all physical wall substrate has thermal conductivity lying between these two extreme correction curves, it can be broadly surmised that the correction curve for a thermally more conducting wall material like aluminum which lies closer to the distribution of $C_{ui}$ as compared to a relatively thermally less conductive wall like perspex should therefore lead to a larger value of critical $Y^+$ ($\equiv Y_c^+$, where wall influence becomes negligible) for the former. Indeed, from numerous works like Chew et al. [12], it is found that $Y_c^+$ for aluminum wall is larger than for the perspex wall counterpart. We shall discuss in a more quantitative manner about $Y_c^+$ in Section 5.4.

### 5.3. Near-wall hot wire correction curves based on Re and $h_0$

The curves of $C_u$ in Fig. 5 is very convenient for experimentalists to correct for the near-wall measured $U_{meas}$ by applying the associated $Y^+$ and $h_0$ to obtain $C_u$ and hence $U_0$ at the hot wire location. The same $C_u$ are next expressed in terms of the usual groupings like $Re$ in Fig. 8 for further elucidation by the fluid dynamists.

From Fig. 8, for the same Reynolds number, the closer the hot wire is to the wall as indicated by smaller $h_0$, the more correction is required for both the adiabatic and isothermal walls. For the same $h_0$, with the increase of Reynolds number, generally $C_u$ will tend towards unity. This is deemed reasonable since for higher $Re$ flow, both the momentum and thermal boundary layers become thinner next to the wall and the heat transfer characteristic of the hot wire behaves more like under free stream condition. For the adiabatic wall, however, $C_{ua}$ approaches 1.0 from above at low $Re$ region, intercept the $C_u = 1.0$ axis to assume a quantity slightly below one and then tends towards unity from below with further increase of $Re$.

The experiments as found in Fig. 12 of Chew et al. [12] gives the plots of $U^+$ versus $Y^+$ for a 5 μm diameter wire at various overheat ratio and wire length $L$ to diameter $D$ ratios near an aluminum wall. We selected the data pertain-

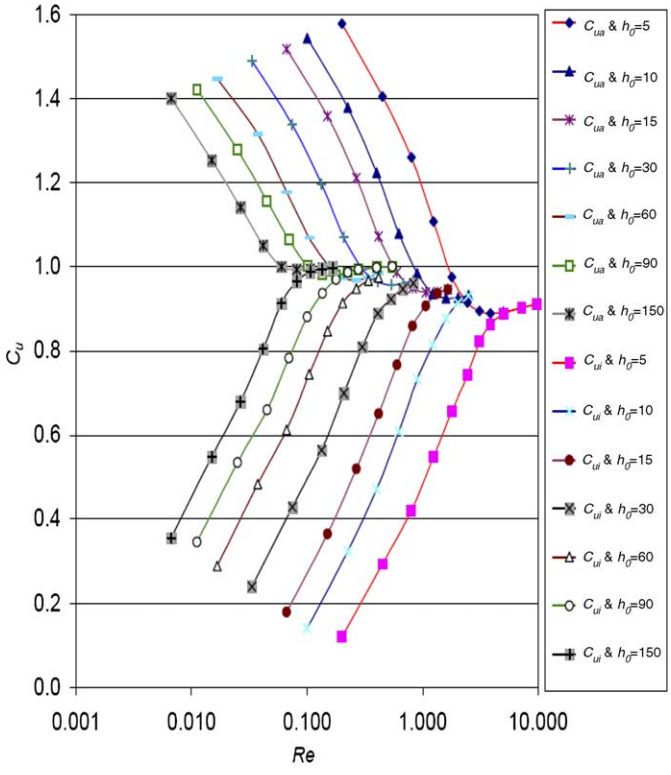


Fig. 8. Variation of $C_u$ with $Re$ and $h_0$ ($\tau = 1.8$).

ing to the overheat ratio of 1.8 and $L/D = 400$ to minimize possible heat loss to the prongs so as to ensure less deviation from two-dimensionality for comparison to our simulation; the said data are reduced to the form of $C_u = f(Re, h_0)$. In Fig. 9, $h_0$ for the experimental data are deduced to be at 10, 12.5, 17, 21, 25, 30, 40 and 60. It is clear that the predicted velocity correction factors are consistent with the corresponding experimental points for $h_0 = 10$, 30 and 60. The simulation provides a lower bound for the experiment at the same $h_0$. The experimental data for $h_0 = 12.5$ fall between the two predicted correction curves for $h_0 = 10$ and 15, the experimental data for $h_0 = 17$, 21 and 25 lie between the two predicted correction curves for $h_0 = 15$ and 30, and the experimental data for $h_0 = 40$ lies between the two predicted curves for $h_0 = 30$ and 60 (Fig. 10).

### 5.4. On the critical $Y_c^+$ and $h_0$

For ease of discussion, we shall define critical $Y_c^+$ as the value of $Y^+$ where the influence of wall takes on a vastly diminishing role for hot wire operating near to the wall. We further define $(Y_c^+)_a$ to be the critical $Y_c^+$ for adiabatic wall while $(Y_c^+)_i$ to be the critical $Y_c^+$ for isothermal wall case. Based on Fig. 5 (data not shown for $Y^+ > 5$), we can obtain $Y_c^+$ by determining the value $Y^+$ where the respective $C_u$ distribution becomes unity within a stipulated margin of $\pm 5\%$ based on the typical experimental uncertainty expected in near-wall measurements. The results of $Y_c^+$ are listed in Table 4.

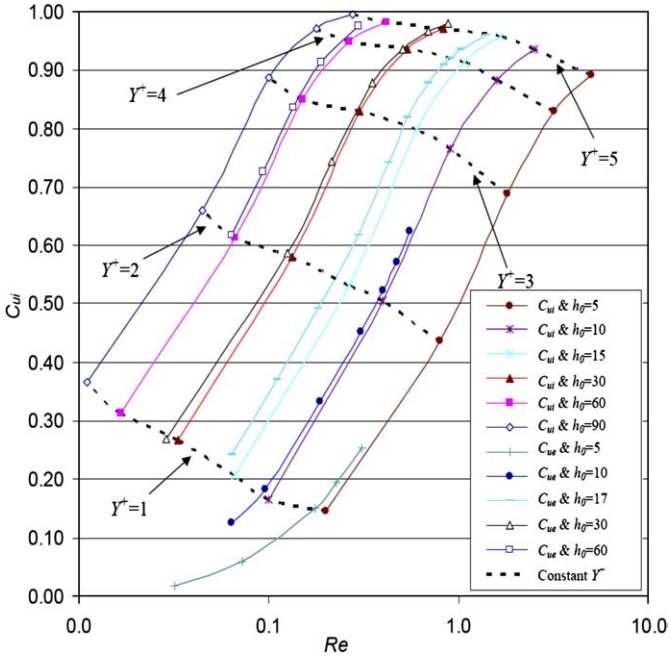


Fig. 10. Variation of $C_u$ with $Re$ and $h_0$ for $\tau = 1.1$ with comparison to experiments $C_{ue}$ [12].

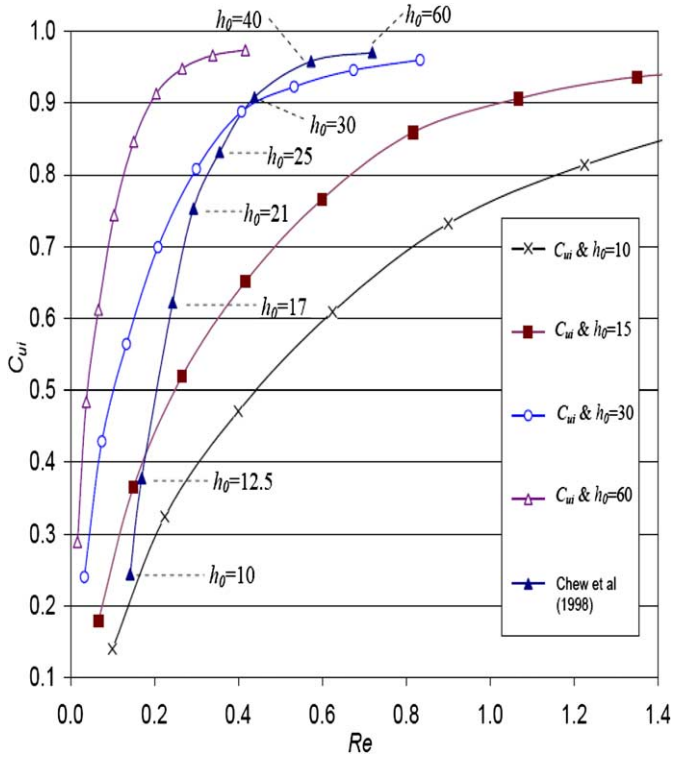


Fig. 9. Variation of $C_u$ with $Re$ and $h_0$ for comparison to experiments [12].

From Table 4, it is clear that with the increase of $h_0$, both $(Y_c^+)_i$ and $(Y_c^+)_a$ are decreasing. This is reasonable since a smaller hot wire diameter should have diminishing influence on the flow and temperature fields. Perhaps what is more surprising (in that it is rather counter-intuitive) is even at $h_0 = 150$, $Y_c^+$ still takes on a quantity larger than 2.0 for either the adiabatic or isothermal wall. That is, the distribution of $Y_c^+$ is only asymptotic towards a null quantity at very large $h_0$. Closer examination suggests this could be the situation since in near-wall hot wire operation, the Reynolds number is very small indeed and accordingly, there is the dominance of the viscous diffusive effect which influence extends much further spatially. (In the usual encounter of flow over much larger scale cylinder at much higher Reynolds number, the inertia effect is dominating and the flow physics associated with it is not directly applicable to the extremely low $Re$ encountered in near-wall hot wire operation.) From Table 4, since both $(Y_c^+)_a$ and $(Y_c^+)_i$

Table 4
Variation of critical $Y_c^+$ with $h_0$

| $h_0$ | 5 | 10 | 15 | 30 | 60 | 90 | 150 |
|---|---|---|---|---|---|---|---|
| $(Y_c^+)_a$ | 2.71 | 2.65 | 2.59 | 2.54 | 2.47 | 2.44 | 2.43 |
| $(Y_c^+)_i$ | 15.8 | 10.2 | 6.30 | 5.02 | 3.53 | 3.12 | 3.12 |

are dependent on $h_0$, it is logical to assume that $Y_c^+$ for any wall substrate material is a function of $h_0$ too.

It may be noted that as $Y_c^+$ were obtained from experiments with air as the working medium and employment of the more traditional wall substrate material (such that the thermal conductivity of the wall is larger than that of air), one can then expect that $Y_c^+ < (Y_c^+)_i$ at the same $h_0$ since isothermal wall can be regarded as infinitely thermal conducting. This notion of $Y_c^+ < (Y_c^+)_i$ follows naturally from the expected (experimental) distribution of $C_u$ versus $Y^+$ assuming a larger magnitude than the corresponding $C_{ui}$ for a given $h_0$ which will then logically 'intersect' the $C_u = 1.0$ at a smaller $Y_c^+$. For any wall substrate with working air medium, one should be aware that for a given $h_0$ though $Y_c^+$ is bounded by $(Y_c^+)_i$ at the upper limit, it is not so for $(Y_c^+)_a$ to serve as the lower limit. This is evident from the $C_{ua}$ distribution taking on a non-monotonically functional form and which crosses the $C_u = 1.0$ axis unlike that found for the $C_{ui}$ distribution (see Fig. 5). For example, Chew et al. [12] found experimentally that $Y_c^+$ for perspex wall takes on a value of 2.1 for their hot wire of 0.63 μm diameter, a quantity smaller than all the computed $(Y_c^+)_i$ and $(Y_c^+)_a$, regardless of $h_0$.

Experimentally, Chew et al. [12] found that the critical $Y_c^+$ for aluminum wall takes on decreasing value of 5.0, 3.7 and 3.0 corresponding to hot wire diameter of 5 μm, 1.27 μm, 0.63 μm, respectively. Although $h_0$ is not provided explicitly, it can be deduced from their Figs. 2, 5 and 7 and evaluated as $h_0 \approx 25$, 50 and 110 for the decreasing hot wire diameter. From the tabulated quantities of $(Y_c^+)_i$ in Table 4 and by fitting a spline curve through the data points, we obtain $(Y_c^+)_i$ as 5.0, 3.9 and 3.1, respectively, for $h_0 = 25$, 50 and 110. These calculated quantities of $(Y_c^+)_i$ are higher than the correspondingly measured critical $Y_c^+$ for the aluminum wall, although it may be mentioned the experiments were based on overheat ratio of 1.1 as opposed to the calculation at $\tau = 1.8$.

Lastly, it may be mentioned that Chew et al. [12] obtained the critical $Y_c^+$ for perspex wall as 3.0, 2.6 and 2.1 corresponding to hot wire diameter of 5 μm, 1.27 μm, 0.63 μm, respectively. From their respective Figs. 4, 6 and 8, it can be deduced that $h_0 \approx 12.5$, 40 and 77.5 for the decreasing hot wire diameter. At the same $h_0$, our evaluated $(Y_c^+)_i$ from the spline curve fitting to the data points from Table 4 give rise to the quantities of 8.8, 4.4, 3.2; all of which are larger than the respective measured counterpart for the perspex wall. This is consistent with the discussion above on $(Y_c^+)_i$ as the upper bound.

### 5.5. On the velocity correction factor, $C_{ui}$, based on overheat ratio of 1.1

As for Section 5.3 on the velocity correction factor based on overheat ratio of 1.8, the computation for overheat ratio $\tau = 1.1$ is carried out for both under free stream and near-wall isothermal conditions to obtain $C_{ui}$. Fig. 10 shows the distribution of $C_{ui}$ with $Re$ for selected $h_0$ with comparison to experiments from Chew et al. [12]. The experiments were deduced from their Fig. 2 for a 5 μm diameter mounted next to the aluminum wall. (We shall use $C_{ue}$ to denote the experiment in the figure.) It is clear from Fig. 10 that the predicted $C_{ui}$ agrees reasonably well by taking on a smaller quantity than the corresponding $C_{ue}$ for $h_0 = 5$, 10, 30 and 60. The experimental data for $h_0 = 17$ falls between the two predicted correction curves for $h_0 = 15$ and 30. On the same figure, the loci for $Y^+ = 1.0$, 2.0, 3.0, 4.0 and 5.0 are provided to give an indication of the proximity to the wall.

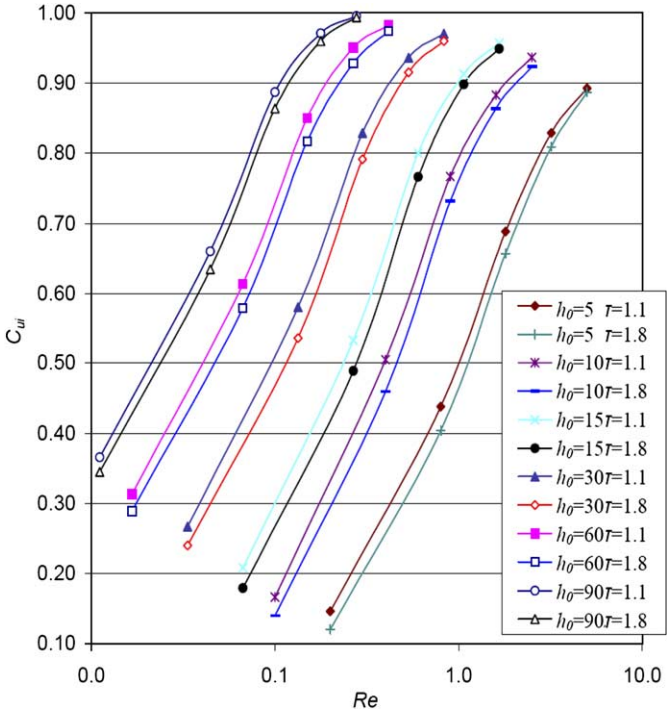


Fig. 11. Variation of $C_{ui}$ with $Re$ and $h_0$ for $\tau = 1.1$ and 1.8.

To investigate the influence of overheat ratio on the velocity correction factor, the variation of $C_{ui}$ with $Re$ and $h_0$ for $\tau = 1.1$ and 1.8 are given in figure for comparison. Fig. 11 shows that the smaller overheat ratio is associated with smaller velocity correction. To further quantify the difference, Fig. 12 shows the variation of $\Delta C_u$ $(\equiv 100\% \times [C_{ui}(\tau = 1.1) - C_{ui}(\tau = 1.8)]/C_{ui}(\tau = 1.8))$ with $Re$ and $h_0$. For the same $h_0$, with the decrease of Reynolds number, $\Delta C_u$ becomes larger. One can also note that $\Delta C_u$ is a function of $h_0$; the smaller the value of $h_0$, the greater the difference at a given $Re$. Lange et al. [2] showed that the velocity correction factor is weakly dependent on the overheat ratio. Their observations seem to be in direct contradiction to our simulation results. It is important to note, however, their conclusion is based on results obtained for $\tau = 1.003$ and 1.27, and there is no mention of the associated value of $h_0$. From Fig. 12, if $h_0$ is large at say 90, the difference is limited to less than 10%. For even larger $h_0$ value, it is expected to diminish further.

From their experiments performed near an aluminum wall with an overheat ratio ranging from 1.06 to 1.8, Krish-

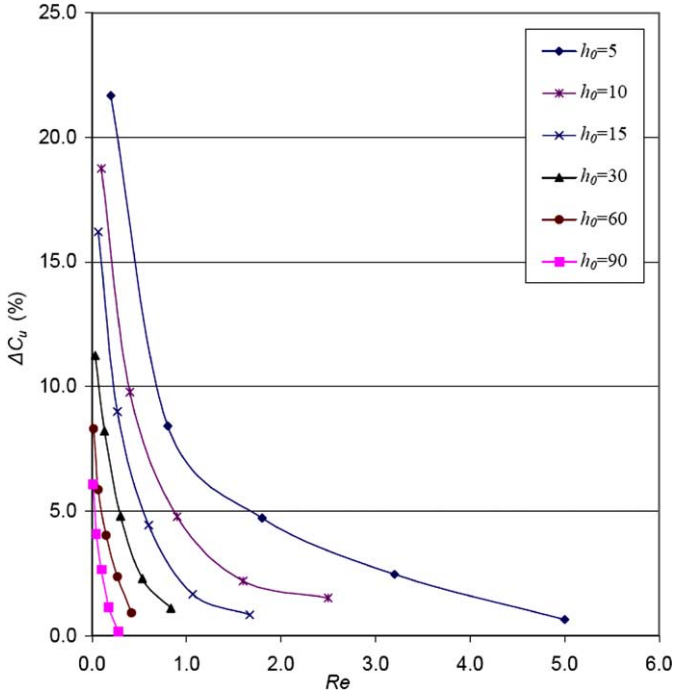


Fig. 12. Variation of $\Delta C_u$ with $Re$ between overheat ratio 1.1 and 1.8.

namoorthy et al. [11] found that generally the deviation of the measured mean $U^+$ distribution from the linear profile of $U^+ = Y^+$ for $Y^+ \leqslant 5$ becomes larger with the use of a larger overheat ratio. This observation is consistent with our simulation result for $\tau = 1.1$ and 1.8. Although the lowest overheat ratio Krishnamoorthy et al. [11] used at $\tau = 1.06$ is different from our lower overheat ratio at $\tau = 1.1$, experimental results from Krishnamoorthy et al. [11] showed that the difference between the $U^+$ distributions for $\tau = 1.06$ and $\tau = 1.1$ is quite negligible.

## 6. Concluding summary

A numerical study of the correction curve for near-wall hot wire measurements under the two extreme cases of isothermal and adiabatic wall conditions was carried out. A summary of the findings are given as follows:

1. A possible reason for the apparent discrepancy between the observed trend of the computed near-wall correction curve of Chew and Shi [1] and Lange et al. [2,14] next to a thermally non-conducting wall can be attributed to the former employment of an insufficiently stringent criterion of convergence set at $10^{-4}$ for $\varepsilon_f$, $\varepsilon_v$. It is found that a more stringent convergence criterion at $10^{-6}$ is needed.
2. For the given isothermal and adiabatic wall conditions, the near-wall correction curve given as $C_u(\equiv \frac{U_0}{U_{\text{meas}}})$ can be expressed in terms of two non-dimensional quantities, namely $Y^+$ $(\equiv \frac{h_0 U_\tau}{\nu})$ and $h_0(\equiv \frac{h}{D})$. Based on these two non-dimensional parameters, the correction factor curves were obtained for $1.0 \leqslant Y^+ \leqslant 5.0$, and $5 \leqslant h_0 \leqslant 150$. The computed results compared well to the experiments of Krishnamoorthy et al. [11] and Chew et al. [12].
3. From the near-wall correction curve, the critical $Y_c^+$ for negligible wall influence on hot wire measurement is obtained for both isothermal wall $(Y_c^+)_i$ and adiabatic wall $(Y_c^+)_a$. Both $(Y_c^+)_i$ and $(Y_c^+)_a$ decrease with increasing $h_0$, and $(Y_c^+)_i$ can also serve as the upper bound for $Y_c^+$ obtained from experiments.
4. It is important to note that the critical $Y^+$ for negligible wall influence on near-wall measurement is also highly dependent on $h_0$ for both the adiabatic and isothermal walls.
5. From the simulation carried out for $\tau = 1.1$ and 1.8, it is found that the influence of overheat ratio on the velocity correction factor may not be negligible. The said influence increases with decreasing $h_0$ and decreasing $Re$.

## Acknowledgement

We wish to acknowledge Professor P. Freymuth from University of Colorado, Boulder for the discussions we had, the interest he has shown in this work and the advice he has given.

## References

[1] Y.T. Chew, S.X. Shi, Wall proximity influence on hot-wire measurements, in: R.M.C. So, C.G. Speziale, B.E. Launder (Eds.), Near-Wall Turbulent Flows, Elsevier, Amsterdam, 1993, pp. 609–619.
[2] C.F. Lange, F. Durst, M. Breuer, Wall effects on heat losses from hot-wires, Int. J. Heat Fluid Flow 20 (1999) 34–47.
[3] A.E. Perry, G.L. Morrison, Static and dynamic calibrations of constant-temperature hot-wire systems, J. Fluid Mech. 47 (1971) 765–777.
[4] P. Freymuth, Frequency response and electronic testing for constant-temperature hot-wire anemometers, J. Phys. E: Sci. Instr. 11 (1977) 705–710.
[5] H. Eckelmann, S.G. Nychas, R.S. Brodkey, J.M. Wallace, Vorticity and turbulence production in pattern recognized turbulent flow structures, Phys. Fluids 20 (1977) S225–S231.
[6] R.A. Antonia, L.W.B. Browne, D.A. Shah, Characteristics of vorticity fluctuations in a turbulent wake, J. Fluid Mech. 189 (1988) 349–365.
[7] J.A.B. Wills, The corrections of hot-wire readings for proximity to a solid boundary, J. Fluid Mech. 12 (1962) 388–396.
[8] S. Oka, Z. Kostic, Influence of wall proximity on hot-wire velocity measurements, DISA Inf. 13 (1972) 29–33.
[9] U.K. Singh, R. Shaw, Hot-wire anemometer measurements in turbulent flow close to a wall, DISA Conf. Fluid Dynamic Measurements, Leicester University Press, 1972, pp. 35–58.
[10] K.S. Hebbar, Wall proximity corrections for hot-wire readings in turbulent flows, DISA Inf. 25 (1980) 15–16.
[11] L.V. Krishnamoorthy, D.H. Wood, R.A. Antonia, A.J. Chambers, Effects of wire diameter and overheat ratio near a conducting wall, Exp. Fluids 3 (1985) 121–127.
[12] Y.T. Chew, B.C. Khoo, G.L. Li, An investigation of the wall effects on hot-wire measurements using a bent sublayer probe, Meas. Sci. Technol. 9 (1998) 67–85.
[13] J.C. Bhatia, F. Durst, J. Jovanovic, Corrections of hot-wire anemometer measurements near walls, J. Fluid Mech. 122 (1982) 411–431.

[14] C.F. Lange, F. Durst, M. Breuer, Correction of hot-wire measurements in the near-wall region, Exp. Fluids 26 (1999) 475–477.
[15] B.G. Van der Hegge Zijnen, Measurement of the velocity distribution in the boundary layer along a plane surface, Thesis, University of Delft, 1924.
[16] D.C. Collis, M.J. Williams, Two-dimensional convection from heated wires at low Reynolds numbers, J. Fluid Mech. 6 (1959) 357–384.
[17] A.F. Polyakov, S.A. Shindin, Peculiarities of hot-wire measurements of mean velocity and temperature in the wall vicinity, Lett. Heat Mass Transfer 5 (1978) 53–58.
[18] A.S. Zemskaya, V.N. Levitskiy, Y.U. Repik, Y.P. Sosedko, Effect of the proximity of the wall on hot-wire readings in laminar and turbulent boundary layers, Fluid Mech.—Sov. Res. 8 (1979) 133–141.
[19] H.H. Bruun, Hot-Wire Anemometry Principles and Signal Analysis, Oxford University Press, 1995.
[20] R.S. Azad, Corrections to measurements by hot-wire anemometer in the proximity of a wall, Report MET-7 Department of Mechanical Engineering, University of Manitoba, Winnipeg, Canada, 1983.
[21] F.M. White, Viscous Fluid Flow, McGraw-Hill, New York, 1991.
[22] J.P. Vandoormaal, G.D. Raithby, Enhancements of the SIMPLE method for predicating incompressible fluid flows, Numer. Heat Transfer 7 (1984) 147–163.
[23] W.Z. Li, Numerical simulations of heat transfer of hot-wire anemometer. Ph.D. thesis, National University of Singapore, 2005.
[24] S.V. Patankar, Numerical Heat Transfer and Fluid Flow, McGraw-Hill, 1980.
[25] W.Z. Li, B.C. Khoo, D. Xu, The thermal characteristics of a hot wire in a fluctuating freestream flow, Int. J. Heat Fluid Flow, submitted for publication.
[26] C.F. Lange, Numerical predications of heat and momentum transfer from a cylinder in crossflow with implications to hot-wire anemometry, Ph.D. thesis, University of Erlangen-Nurnberg, Erlangen, Germany, 1997.
[27] C.F. Lange, F. Durst, M. Breuer, Momentum and heat transfer from cylinders in laminar crossflow at $10^{-4} \leqslant Re \leqslant 200$, Int. J. Heat Mass Transfer 41 (1998) 3409–3430.
[28] Y.T. Chew, S.X. Shi, B.C. Khoo, On the numerical near-wall corrections of single hot-wire measurements, Int. J. Heat Fluid Flow 16 (1995) 471–476.